OAK RIDGE NATIONAL LABORATORY LIBRARIES

3 4456 0570508 3

K/CSD/TM-59
Dist. Category UC-95C

MARTIN MARIETTA

- 2-D laminar flow
- Ht trans. through wall studs ignored.
- About 1/2 heat trans. thru cavity is by radiation.
- adding reflective foil behind wallboard reduces ht trans. across cavity by ~1/2
- Need to keep the convective ht trans component low, i.e. minimize convective flow.

CALCULATION OF HEAT FLUX THROUGH A WALL CONTAINING A CAVITY — COMPARISON OF SEVERAL MODELS

J. E. Park
J. R. Kirkpatrick
J. N. Tunstall
K. W. Childs

FEBRUARY 1986

OPERATED BY
MARTIN MARIETTA ENERGY SYSTEMS, INC.
FOR THE UNITED STATES
DEPARTMENT OF ENERGY

Printed in the United States of America. Available from
National Technical Information Service
U.S. Department of Commerce
5285 Port Royal Road, Springfield, Virginia 22161
NTIS price codes—Printed Copy: A03 Microfiche A01

This report was prepared as an account of work sponsored by an agency of the United States Government. Neither the United States Government nor any agency thereof, nor any of their employees, makes any warranty, express or implied, or assumes any legal liability or responsibility for the accuracy, completeness, or usefulness of any information, apparatus, product, or process disclosed, or represents that its use would not infringe privately owned rights. Reference herein to any specific commercial product, process, or service by trade name, trademark, manufacturer, or otherwise, does not necessarily constitute or imply its endorsement, recommendation, or favoring by the United States Government or any agency thereof. The views and opinions of authors expressed herein do not necessarily state or reflect those of the United States Government or any agency thereof.

By acceptance of this article, the publisher or recipient acknowledges the U.S. Government's right to retain a non-exclusive, royalty-free license in and to any copyright covering the article.

K/CSD/TM-59
Dist. Category UC-95C

CALCULATION OF HEAT FLUX THROUGH A WALL CONTAINING A CAVITY - COMPARISON OF SEVERAL MODELS

J. E. Park
J. R. Kirkpatrick
J. N. Tunstall
K. W. Childs

February 1986

COMPUTING AND TELECOMMUNICATIONS DIVISION
at
Oak Ridge Gaseous Diffusion Plant
Post Office Box P
Oak Ridge, Tennessee 37831

Martin Marietta Energy Systems, Inc.
operating the
Oak Ridge Gaseous Diffusion Plant . Oak Ridge National Laboratory
Oak Ridge Y-12 Plant . Paducah Gaseous Diffusion Plant
Under Contract No. DE-AC05-84OR21400
for the
U. S. Department of Energy

CONTENTS

	Page
LIST OF FIGURES	v
LIST OF TABLES	vii
ABSTRACT	ix
1. INTRODUCTION	1
2. REVIEW OF MODEL AND ALGORITHM	3
3. THE PROBLEM	7
4. PRESENTATION OF NUMERICAL RESULTS	11
5. DISCUSSION OF HEAT TRANSFER RESULTS	13
6. CONCLUSIONS	21
ACKNOWLEDGMENTS	23
REFERENCES	25
Appendix. DESCRIPTION OF THE MODELS USED TO CALCULATE BOUNDARY TEMPERATURES AND HEAT TRANSFER FROM THE AMBIENT TO THE WALL CAVITY	27

LIST OF FIGURES

Figure		Page
1.	Schematic of a standard ASHRAE building wall	4
2.	Streamlines for a cavity bounded by conducting, radiating walls	12
3.	Isotherms for a cavity bounded by conducting, radiating walls	12
4.	Temperature and heat flux distribution on inner walls of an isothermal cavity	14
5.	Temperature and heat flux distribution on inner walls of an ASHRAE wall structure without top/bottom sill plates	15
6.	Temperature and heat flux distribution on inner walls of an ASHRAE wall structure without radiative transport	16
7.	Temperature and heat flux profiles on inside surfaces of an ASHRAE wall cavity	17
8.	Temperature and heat flux profiles on inside surfaces of an ASHRAE wall cavity with foil liner added	19
A.1.	Schematic of thermal resistance network showing coupling from gas to cavity and ambient temperatures	28

LIST OF TABLES

Table		Page
Table 1.	Description of cases modeling heat flow through a hollow wall cavity	7
Table 2.	Thermal resistance used to calculate heat transfer through a wall cavity	8
Table 3.	Fluid properties and non-dimensional groupings	9
Table 4.	Total energy transfer rate through the wall system	11

ABSTRACT

This paper describes the calculation of the heat transfer through the standard stud wall structure of a residential building. The wall cavity contains no insulation. Results from five test cases are presented. The first four represent progressively more complicated approximations to the heat transfer through and within a hollow wall structure. The fifth adds the model components necessary to severely inhibit the radiative energy transport across the empty cavity.

Flow within the wall cavity is calculated from the Navier-Stokes equations and the energy conservation equation for an ideal gas using an improvement to the Implicit-Compressible Eulerian (ICE) algorithm of Harlow and Amsden. An algorithm is described to efficiently couple the fluid flow calculations to the radiation-conduction model for the solid portions of the system.

The results indicate that conduction through sill plates contributes less than 2% of the total heat transferred through a composite wall. All of the other elements (conduction through wall board, sheathing, and siding; convection from siding and wallboard to ambients; and radiation across the wall cavity) are required to accurately predict the heat transfer through a wall. Addition of a foil liner on one inner surface of the wall cavity reduces the total heat transferred by almost 50%.

1. INTRODUCTION

Natural convection in rectangular cavities has been the subject of scientific and engineering interest for a number of years. For example, the heat transferred across the hollow cavities between the exterior sheathing and the interior panel of a building wall represents an important component of the energy costs of heating or cooling buildings. Experimental studies reported by Catton (ref. 1) give an idea of the complexity of the problem. Numerical simulations have been done by a number of investigators with rather varied results. For example, De Vahl Davis and Jones (ref. 2) compare the results of various calculations, using different methods. For one value of Raleigh number (10^5, the same order of magnitude as for the flows considered in this paper), the prediction for peak heat flux varied from 190% to 95% of the correct value on the single problem of flow in a square cavity with isothermal walls. This range of answers should instill a certain humility in the attitudes of numerical fluid dynamicists.

The computational approach, however, has several advantages. Physical experiments (as opposed to numerical experiments) are very difficult with fluids of interest such as air. Water is relatively easy to use for experiments, but the scaling laws from water to air span a wide range of Raleigh numbers. That is, for values of temperature difference which can be conveniently used in the laboratory, the balance between convection and conduction is much different when using water than when using air. The proper numerical algorithm, on the other hand, can simulate either fluid relatively easily for many conditions. Thus many numerical experiments can be run inexpensively with only occasional experimental verification required.

This report documents a study of heat transfer through a building wall which is typical of residential construction. For this study, the cavity between the exterior sheathing and interior panel does not contain any insulation. While the omission of insulation is not considered a good building practice by modern standards, many houses have been built this way in the past. Documentation of this study serves at least two purposes. The first is to demonstrate the validity of the calculation method. Once the algorithm has been shown to give results which match results for this configuration from elsewhere in the literature, the algorithm may be used for other configurations with some confidence. Because experiments measuring heat transfer in cavities are expensive, a method which can be used to calculate such heat transfer should be a valuable contribution to the science. A second purpose for documenting this study is that the results represent a baseline for comparison with the results of studies of heat transfer using other numerical methods.

2. REVIEW OF MODEL AND ALGORITHM

The objective of this report is to calculate the heat flow through the wall structure from the hot ambient on one side to the cold ambient on the other. Details of the fluid motion and temperature within the cavity are an important part of that calculation.

The geometric configuration is sketched in Fig. 1. A section of a standard residential wall is shown. Starting from the inside (left), the wall consists of gypsum wallboard, the empty cavity (which, in modern construction, would be filled with insulation), a layer of sheathing, and wood siding which is exposed to the outside air. The cavity is enclosed at top and bottom by wooden sills.

In the structural parts of the wall, the standard heat conduction equation, with constant thermal conductivity, is assumed to govern. In this work, the conduction of energy from hot to cold ambients through the studs is ignored. With that simplification, the problem which remains is presumed to be two-dimensional. That is, air circulation and heat conduction into or out of the plane of Fig. 1 are neglected. Thermal radiation exchange between the interior surfaces of the cavity is described using the Stefan-Boltzman equation and assuming that those surfaces are "gray bodies." Thermal boundary layers between the room ambient and the gypsum board and the outside ambient and the wood siding are represented by constant values for thermal resistance taken from the literature.

The technique used to calculate the radiant interchange and the heat flow through the solid portions of the wall and the coupling of the fluid calculation to the ambient temperature boundary conditions is discussed further in the appendix.

The fluid motion in the cavity is governed by the Navier-Stokes equations (Newton's Second Law applied to a fluid). These are solved numerically, along with the conservation laws for mass and energy. In calculating the fluid motion, the most important assumptions made are that the transport properties (specific heat, viscosity, and thermal conductivity) are constant; that the fluid motion is laminar; and that the viscous dissipation of mechanical energy can be neglected. The fluid within the cavity (air) is presumed to obey the ideal gas equation of state.

Mathematically, the physical laws are expressed as four nonlinear partial differential equations. The dependent variables are the horizontal and vertical velocities, the pressure and the temperature throughout the cavity. The density can be calculated from the pressure and temperature using the equation of state.

The partial differential equations describing the fluid motion are solved using a well established finite difference algorithm, the Implicit Compressible Eulerian (ICE) technique due to Harlow and Amsden (refs. 3,4). The equation describing the steady-state temperature in the solid portions is solved using a lumped parameter technique described in the appendix. The finite difference equations approximating the fluid motion are marched forward in time, developing a numerical description of the transient fluid motion. The steady-state values for the solid temperatures on the cavity edges are calculated at each time step, driving the solution toward a steady-state answer more rapidly than a fully transient solution. Since

DWG. NO. K/G-85-5512
(U)

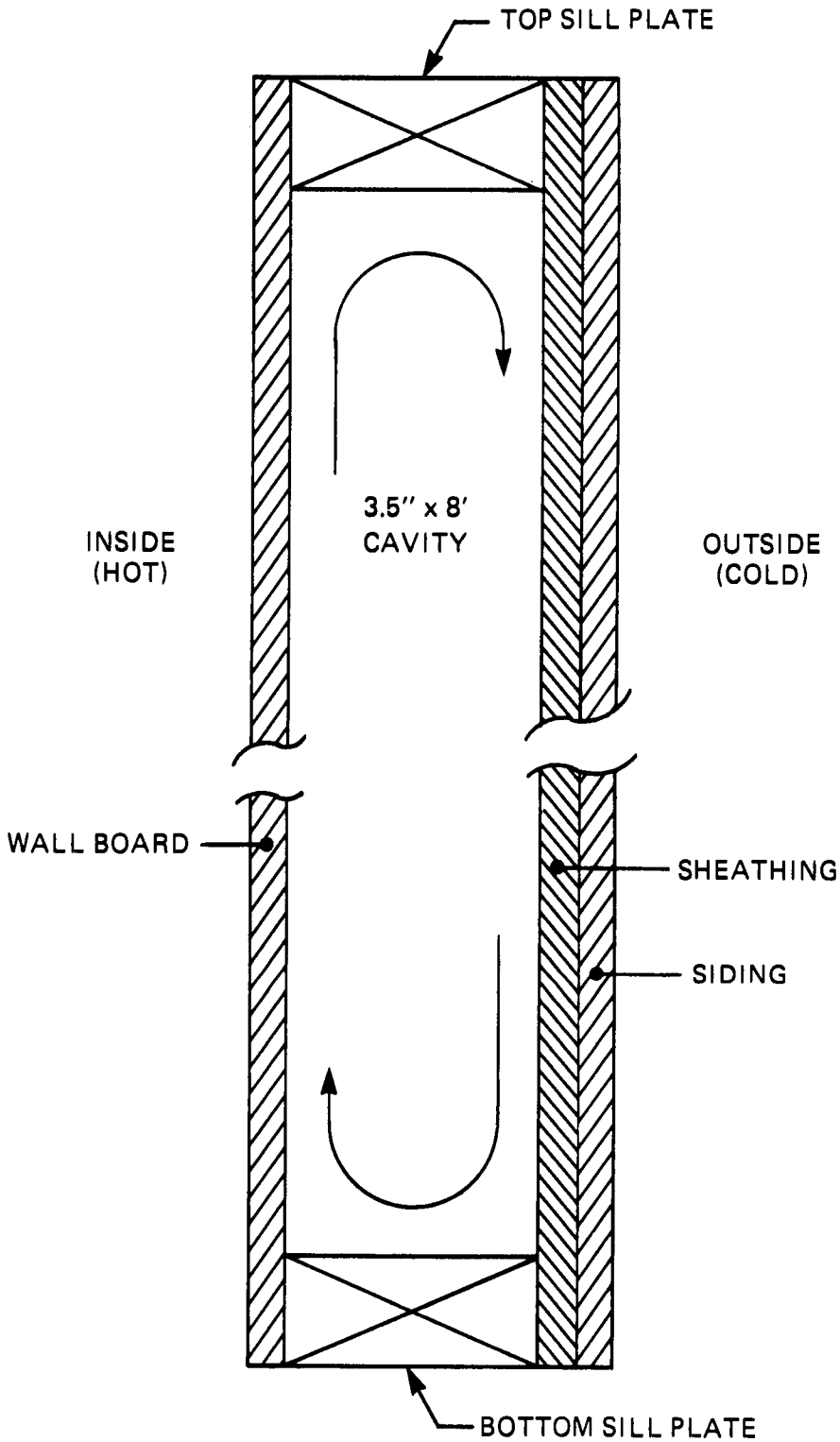

Fig. 1. Schematic of a standard ASHRAE building wall.

the ultimate boundary conditions (the bounding temperatures from the environment) are constant, the calculated fluid velocities eventually reach a steady state. Calculations are stopped and the results analyzed when an overall heat balance has been achieved and the fluid motion has reached a steady state.

3. THE PROBLEM

Five separate cases have been evaluated using the numerical model summarized above. The first four represent progressively more complicated approximations to the heat transfer through and within a hollow wall structure. The fifth adds the model components necessary to severely inhibit the radiative energy transport across the empty cavity. These cases are summarized in Table 1.

Table 1. Description of cases modeling heat flow through a hollow wall cavity

Case No.	Title	Description
1	Isothermal Walls	The temperature of the inner wall is fixed at 540R; the outside wall is fixed at 530R.
2	Conducting walls	Film resistances for boundary layers are added at the outer edges of the wall materials; heat conduction through the wall is calculated.
3	Case 2 with sills	Heat conduction through the sill plates at top and bottom and conduction between gas and sills are added.
4	Case 3 with radiation	Thermal radiation between inner surfaces across the cavity is added.
5	Case 4 with foil backing	A foil backing (high reflectivity) is added to one surface of the cavity to cut radiant transfer.

For the most simple case, the natural convection within the empty cavity, bounded by the exterior sheathing and the interior wallboard, is calculated assuming that the sheathing is at a uniform temperature and that the wallboard is at a different uniform temperature. No heat transfer is allowed from the air in the cavity to the sills at the top and bottom of the cavity. For the second case, the uniform temperatures are assigned to the ambient air on either side of the wall structure. Conduction through the exterior siding and the interior paneling, and convection across the boundary layers between the siding and paneling and their respective ambient air temperatures, are added to the heat transfer path. For the third case, conductive paths are added from the cavity to the ambient air

temperatures through the sill plates at the top and bottom of the wall. For the fourth case, radiant heat transfer within the cavity is added to the calculation. Finally, in the fifth case, reflective foil is added to the inside wall panel. For each model, wall temperature profiles, wall heat flux profiles, and integrated total heat flow rates are presented.

The wall structure used in these calculations was the standard wall defined in ref. 5. Dimensions and thermal conductivities are given in Table 2. The configuration is sketched in Fig. 1.

Table 2. Thermal resistance used to calculate heat transfer through a wall cavity *

Component	Resistance (sq ft-hr-R/Btu)	Thickness (ft)
Inside surface (still air)	0.68	-
Gypsum wallboard panel	0.45	0.0417
Reflective liner (Case 5 only)	0.00	-
Sheathing	1.32	0.0417
Wood siding	0.81	0.0417
Outside surface (15 mph wind)	0.17	-

* Taken from ref. 5, p. 22.18, Table 4A.

The exterior siding is backed by a sheathing material. This exterior laminate is separated from the interior wall by an air cavity the width of stud spacers. The interior wall is gypsum wallboard. Conduction through the vertical studs is neglected, although conduction through timber plates at the top and bottom of the cavity is included in the last three versions of the model. Heat transfer coefficients between the ambients (exterior and interior) and the wall composite are as prescribed by the American Society of Heating, Refrigeration and Air Conditioning Engineers (ASHRAE) Guide (ref. 5).

For a finite difference mesh of 25 cells in the horizontal direction by 48 cells in the vertical direction, about 15 min. of CPU time (IBM 3033 system), 2500 time steps, were required to reach a steady state. The mesh was nonuniform in both the horizontal and vertical directions, with computational cells concentrated in the boundary layers near the solid surfaces.

For all calculations, an overall temperature difference of 10°F was imposed. Values for physical parameters and the usual nondimensional groupings are given in Table 3.

Table 3. Fluid properties and non-dimensional groupings

Property	Value
Nominal pressure (lb_f/sq. ft.)	2132.017
Specific heat (c_p, Btu/R-lb_m)	0.24
Thermal conductivity (Btu/ft-R-s)	4.25×10^{-6}
Viscosity (lb_m/ft-s)	3.841×10^{-7}
Temperature of hot ambient (R)	540.0
Temperature of cold ambient (R)	530.0
Emissivity of wallboard	0.93
Emissivity of sheathing	0.93
Emissivity of reflective foil	0.05
Prandtl number	0.698

4. PRESENTATION OF NUMERICAL RESULTS

Results of the five cases are presented and compared in this section. Plots of streamlines and air temperature contours are presented for the fourth problem (Figs. 2,3). Wall heat flux and wall temperature values are presented for each problem. Integral quantities (overall heat flow rate, thermal resistance) are presented in Table 4.

Figure 2 displays the streamlines for the fourth (and most realistic) problem. The left wall is the hot wall. Streamlines separate channels containing equal mass flow rates. In Fig. 2, each channel carries 3.3×10^{-4} lb_m/ft-s of mass flow. The direction of circulation is indicated by the arrow on the plot. As expected, the fluid rises on the hot (left) wall and falls on the right (cool) wall.

Figure 3 shows the isotherms for the fourth case. The isotherms are plotted for 1°R increments. If the fluid were not circulating, these isotherms would be vertical lines spaced equally between the two walls. The circulation, however, has carried hot fluid to and along the upper sill. The heat transfer from the air to the sills is rather small so that air flowing near the upper sill is very nearly at the temperature of the inner (left, hot) wall. Similarly, the cold fluid on the outer (right, cold) wall is carried along the bottom sill so that the temperature of the outer wall is virtually the same as that of the right wall.

The total energy transferred through the wall system, and the corresponding R values for the various problems are shown in Table 4. The maximum stream function value, a measure of the circulation rate, is also tabulated. The R value is calculated by dividing the product of wall area (8 ft) and overall temperature difference (10°F) by the heat flow in Table 4.

Table 4. Total energy transfer rate through the wall system

Case No.	Description	Heat flow, (Btu/ft-s)	R Value (sq ft-hr-R/Btu)	Circulation rate (lb_m/ft-s)
1	Isothermal Walls	4.09×10^{-3}	5.43	3.18×10^{-3}
2	Conducting walls	2.45×10^{-3}	9.03	2.30×10^{-3}
3	Case 2 + sills	2.53×10^{-3}	8.77	2.34×10^{-3}
4	Case 3 + radiation	5.15×10^{-3}	4.31	1.82×10^{-3}
5	Case 4 + foil backing	2.94×10^{-3}	7.55	2.31×10^{-3}

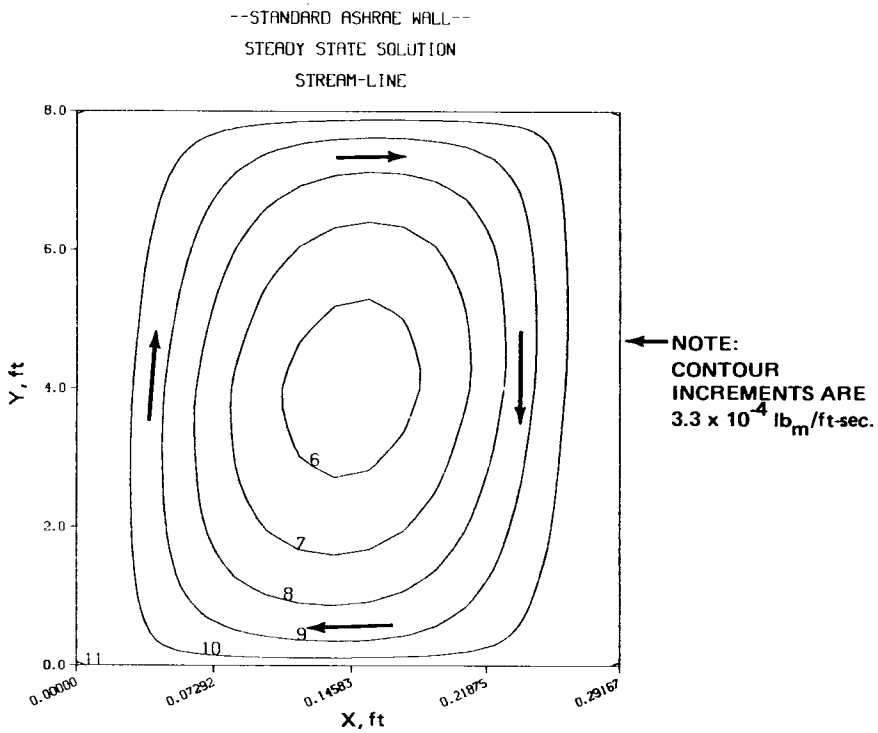

Fig. 2. Streamlines for a cavity bounded by conducting, radiating walls.

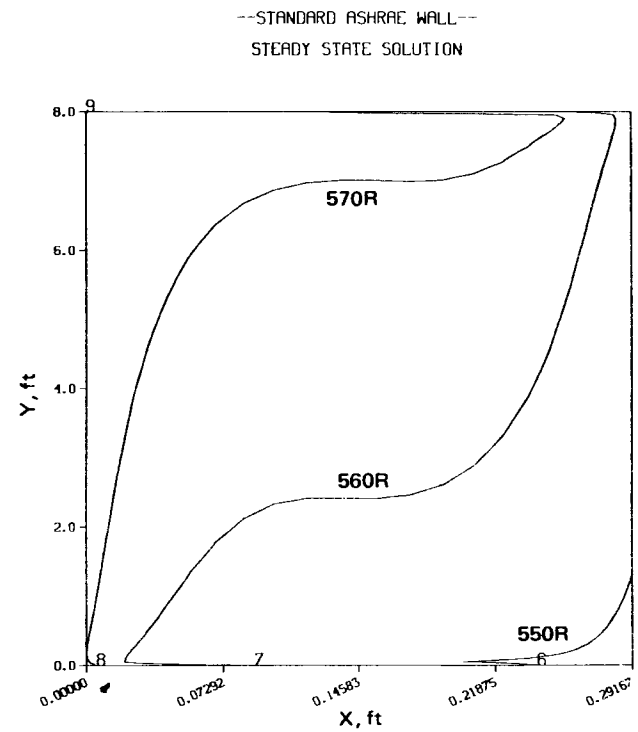

Fig. 3. Isotherms for a cavity bounded by conducting, radiating walls.

5. DISCUSSION OF HEAT TRANSFER RESULTS

In this section, numerical temperature and heat flux solutions are presented for each of the five cases. In each case, an ambient temperature, a wall temperature, and a gas temperature 0.025 ft from the wall are presented as functions of distance above the bottom sill. For the first case, the wall temperature and the ambient temperature coincide so that only one curve appears. Similarly, local heat fluxes along the vertical cavity surfaces are plotted against the height above the sill. For cases 4 and 5, both convective and total heat fluxes are plotted so that the magnitude of the radiative transport can be observed. All five cases exhibit rapid change in temperature and heat flux near the corners of the cavity. These phenomena result from flow stagnation or formation of small eddies in the corners.

The first case is an idealized problem. The only resistance to heat flow through the cavity is that of the air in the cavity. Since the convection tends to pump heat from the hot wall to the cold wall, the effective resistance is much less than that for pure conduction. Examination of Fig. 4 reveals that the heat flow is not uniform. Much of the heat enters the cavity at the bottom of the hot wall and leaves through the top of the cold wall. This, of course, is a consequence of the thickening of the boundary layers in the direction of flow. McAdams (ref. 6, p. 181, Eqs. 7-9b) recommends a correlation for heat transfer under these conditions which gives a resistance of about 5.5 sq ft-hr-R/Btu. This is consistent with the value of 5.43 from Table 4.

For the second case, ASHRAE values for thermal resistance for the vertical walls and convective coefficients for the ambient conditions are added to the model. As expected, the heat flow rate is reduced as resistance to the heat flow is added (Table 4). Heat flux and temperature profiles along the cavity walls are shown in Fig. 5.

For the third case, sill plates above and below the cavity are added as parallel conduction paths. As can be seen from Table 4, and by comparing Figs. 5 and 6, the effect of these on the overall heat transfer is slight (less than 3%). The small increment of heat transfer added by the sills is not surprising. The top and bottom sill structures have less than 4% of the the total cavity surface area. In addition, the heat path from the gas-sill interfaces, through the sill plates to the ambient, has a higher resistance than the path across either wall to the ambients.

The fourth problem represents the most complete model of the ASHRAE wall. Realistic values for radiant energy transport parameters were used, along with the sill models and conduction-convection parameters from the third case. From Table 4, the parallel energy transfer due to radiation increases the heat transfer through the wall significantly. The calculated overall R value of 4.31 from the table compares well with the value given by the ASHRAE Tables (R = 4.44), establishing some confidence in both the tabulated value and the present calculations. Figure 7 shows the temperature and heat flux profiles for this solution.

The differences between the third and fourth cases illustrate how important radiant heat transfer is for an uninsulated wall. Adding radiant heat transfer doubles the total heat flow. Looking at the heat flow results in Table 4, one might be tempted to say that the convective path

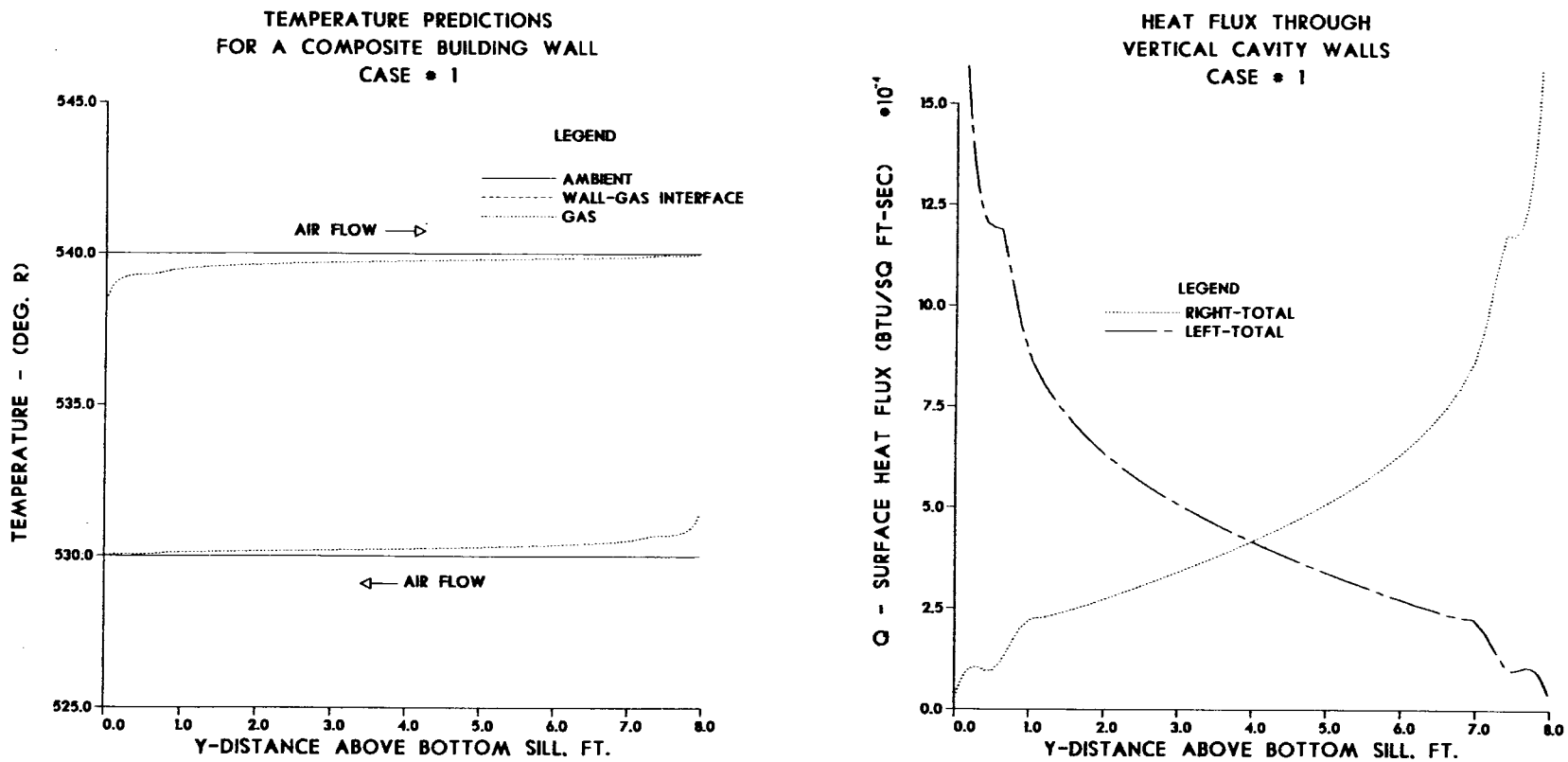

Fig. 4. Temperature and heat flux distribution on inner walls of an isothermal cavity.

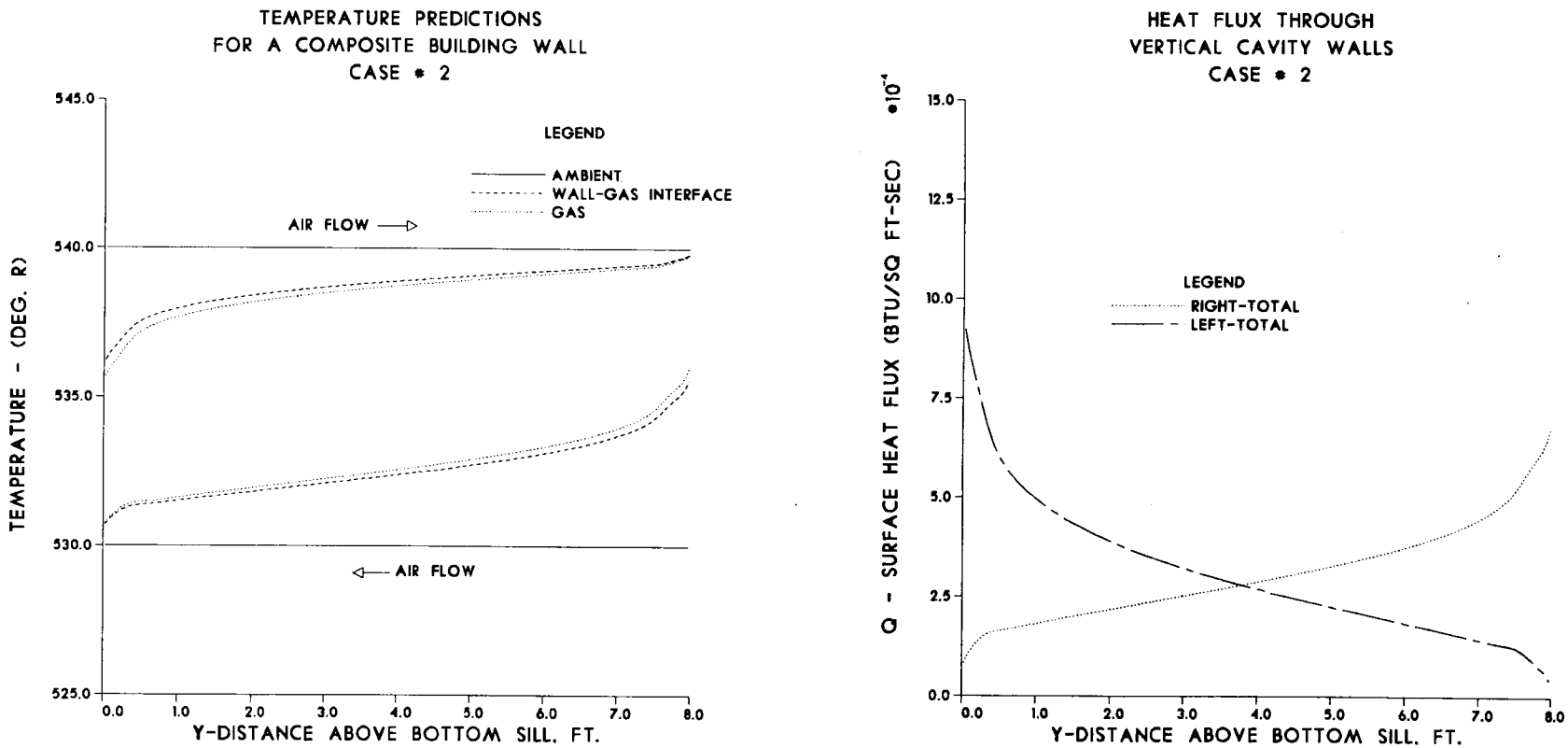

Fig. 5. Temperature and heat flux distribution on inner walls of an ASHRAE wall structure without top/bottom sill plates.

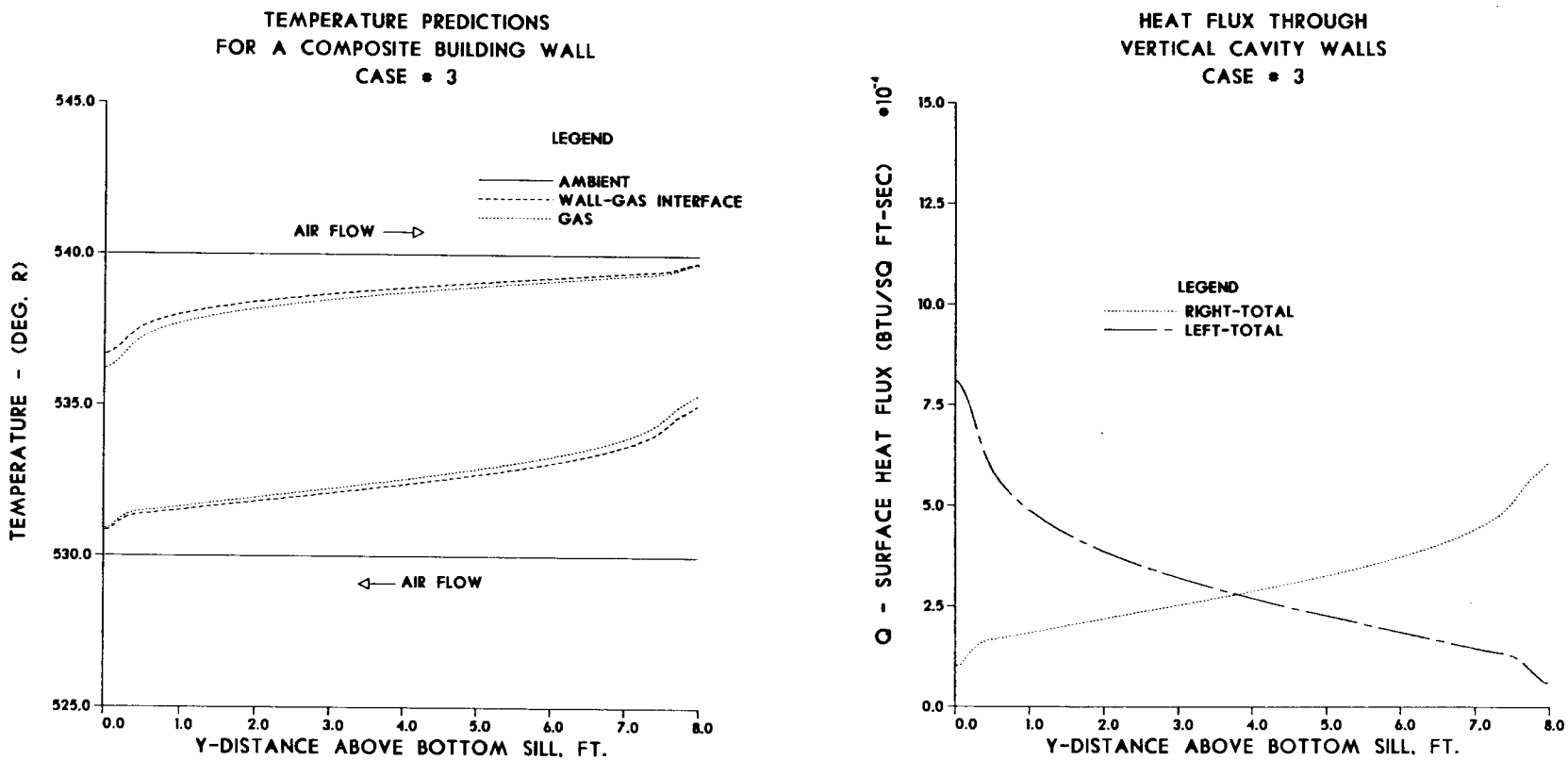

Fig. 6. Temperature and heat flux distribution on inner walls of an ASHRAE wall structure without radiative transport.

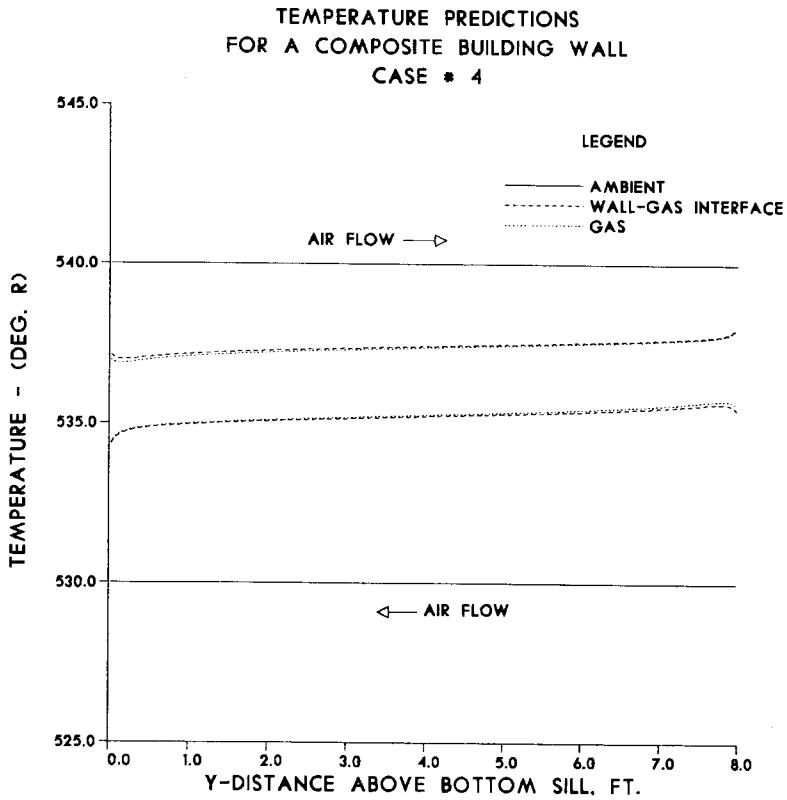

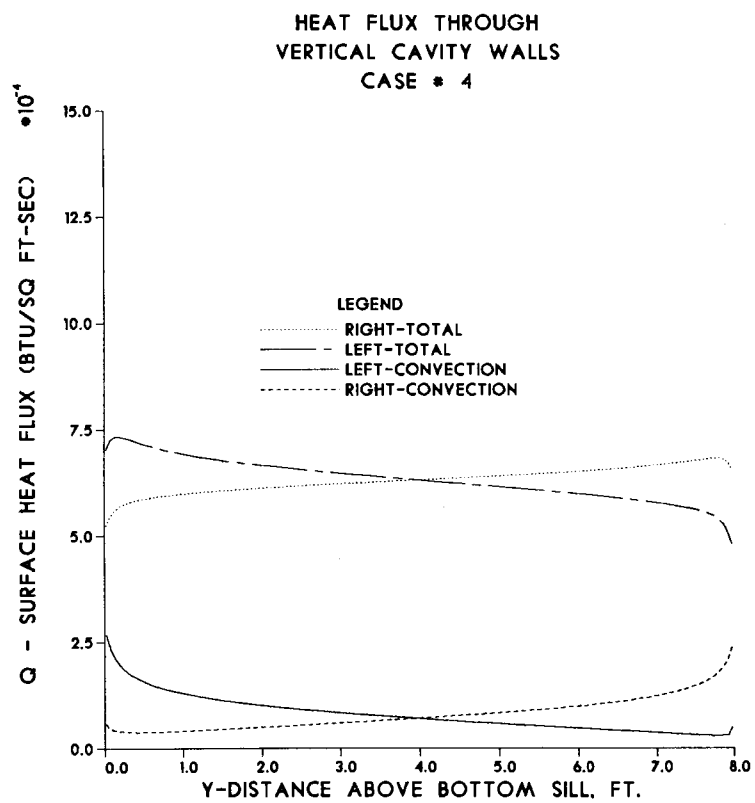

Fig. 7. Temperature and heat flux profiles on inside surfaces of an ASHRAE wall cavity.

across the cavity carries about 2.6×10^{-2} Btu/ft-s, and the radiant path carries approximately the same amount. The truth is more complicated. An examination of Figs. 6 and 7 shows that the differences between wall-gas interface temperatures on the right and left are reduced by a factor of more than 3 by adding the radiant path and that the convective heat fluxes are reduced by an even larger amount. Integrating the curves of heat flux from Fig. 7 gives a total radiant heat transfer of about 4.5×10^{-3} Btu/ft-s and a total convective heat transfer of about 0.6×10^{-3} Btu/ft-s. For the fifth case where the emissivity of the paneling was reduced to 0.05 (from 0.93), the total radiant heat transfer is about 0.8×10^{-3} Btu/ft-s with a total convective heat transfer of about 2.1×10^{-3} Btu/ft-s.

Some additional conclusions can be drawn by comparing the results from the third and fourth cases. Radiant heat transfer and conductive heat transfer are parallel paths. These two mechanisms have individual heat transfer coefficients which are of comparable magnitudes; thus, an insulation which is to achieve a high resistance across the cavity must decrease the heat transfer due to both. By neglecting heat transfer through the sills and subtracting all other R values (Table 2) from the total given in Table 4, an R value for the cavity can be calculated. From the results for the third case, an insulation that suppresses all radiant heat transfer but leaves the convection undisturbed gives an air gap resistance of about 5.4 sq ft-hr-R/Btu. For the fourth case, the radiant heat transfer dominates the total heat flow. The air gap resistance for this case is about 1.0 sq ft-hr-R/Btu. As one test of the computer code, a heat transfer rate was calculated for the same conditions as the fourth case but allowing only radiation in the air gap. This test gave a cavity resistance of about 1.1 sq ft-hr-R/Btu. Clearly, an insulation which eliminates convection in the cavity while leaving the radiant heat transfer path undisturbed will gain almost nothing in air gap resistance over an uninsulated wall. On the other hand, while an insulation which eliminates radiant heat transfer without limiting the convective heat transfer will gain in insulating power, the gap resistance is much less than the rated thermal resistance of commercially available foil-faced fiberglass insulations. Thus, the most effective strategy is to inhibit both mechanisms of energy transport.

In the fifth problem, a piece of "foil" (emissivity = 0.05) was added to the model in an attempt to reduce the radiant heat transfer. The foil was laminated to the face of the inside wall of the cavity. The conductive resistance of the foil was ignored. In contrast to the first four models, which were successively more complex and realistic approximations to an actual wall design, this problem is an attempt to improve the thermal performance of the ASHRAE wall by modifying it. Again, from Table 4, the overall heat transfer was reduced significantly by installing the reflective foil. Since the heat flow for case 5 is higher than that for case 3, it is evident that some radiant heat transfer still occurs. Temperature and heat flux profiles are shown in Fig. 8. The resistance of the cavity for this case (calculated as described in the previous paragraph) is about 4.1 sq ft-hr-R/Btu. For comparison, the ASHRAE Guide (ref. 5) suggests an R value for the foil lined air gap of between 3.7 and 3.9.

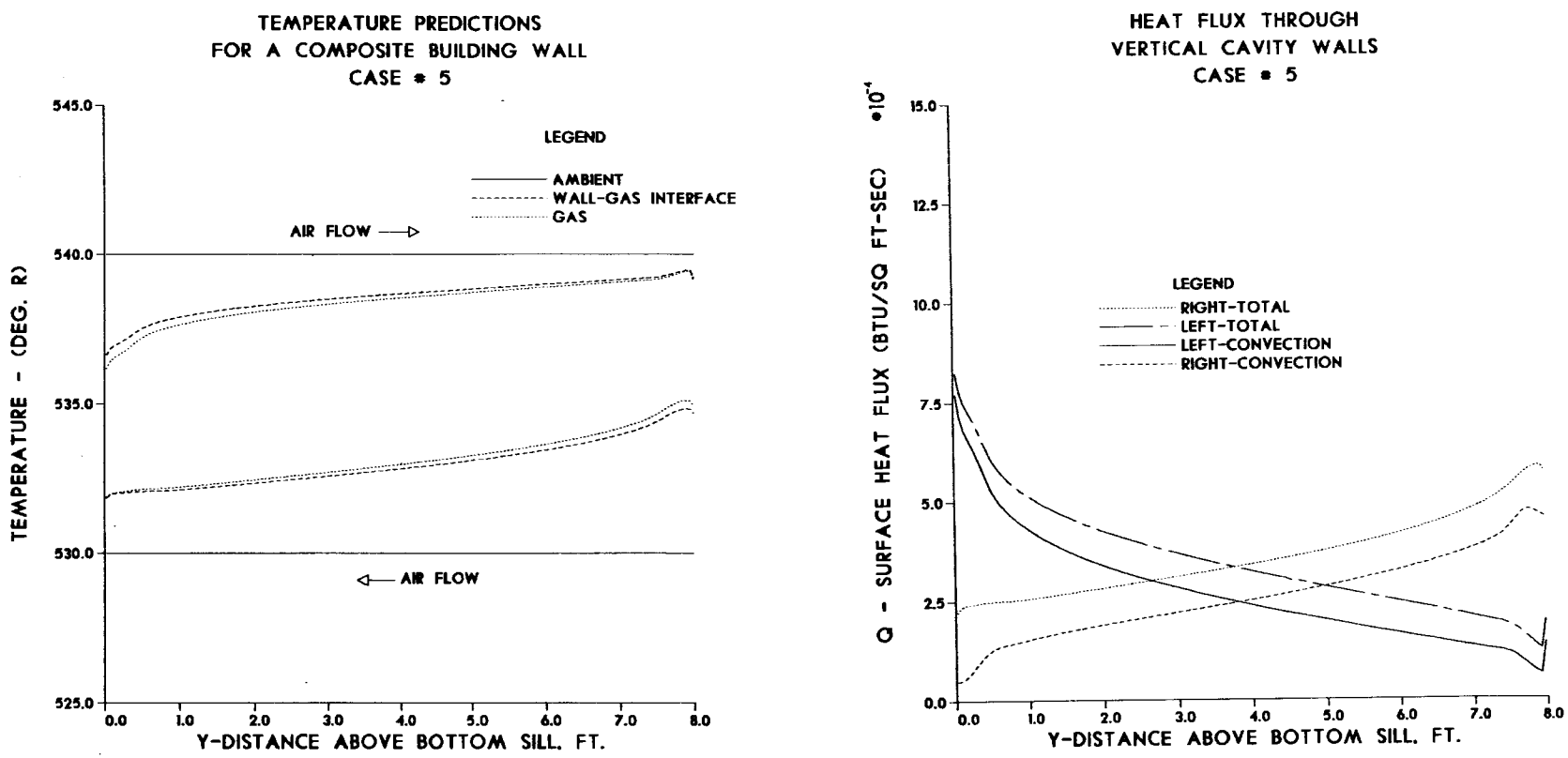

Fig. 8. Temperature and heat flux profiles on inside surfaces on an ASHRAE wall cavity with foil liner added.

6. CONCLUSIONS

The following conclusions are supported by the work reported in this paper.

1. The convective heat transfer calculation algorithm used on the "isothermal wall" configuration yields a heat transfer rate which is within 1.5% of that given by McAdams' correlation of experimental data (ref. 6). Further, calculations of real wall configurations, including radiation heat transfer with and without a foil liner, yield heat transfer rates that are within 3% of industry accepted values published in the ASHRAE guide. These successful comparisons lead to increased confidence both in the numerical technique used in this report and in the published results to which the comparisons are made.

2. The thermal resistance of the vertical wall materials must be included in an accurate model of the entire wall system; use of constant-temperature walls leads to falsely high predictions for heat loss through the wall system. Further, the isothermal approximation does not reveal the substantial temperature differences which develop between the top and bottom of the wall system.

3. Timber sills conduct less than 2% of the energy transferred by the uninsulated wall cavity which they bound.

4. For the uninsulated cavity, thermal radiation is an important transport mechanism even with modest temperature differences.

5. Use of a reflective backing on one face of the wall cavity reduces overall heat transfer by half. Even if the emissivity could be maintained at a low value, bringing the wall up to the values of thermal resistance usually seen in modern, high quality construction will require a considerable degree of control on the convective heat transfer as well.

ACKNOWLEDGMENTS

The work presented in this report was done as a part of the National Program for Building Thermal Envelope Systems and Materials. The research was sponsored by the Office of Buildings and Community Systems, Building Division, U.S. Department of Energy.

The patience and skill of Roger Wallace is evident in the figures contained in this report. The efforts of Irene Rose in converting a draft into a final report are appreciated.

REFERENCES

1. Ivan Catton, "Natural Convection in Enclosures," Proceedings of the Sixth International Heat Transfer Conference, vol. 6, pp. 13-32, August 1978.

2. G. De Vahl Davis and I. P. Jones, "Natural Convection in a Square Cavity," Proceedings of the Second International Conference on Numerical Methods in Thermal Problems, July 7-10, 1981, Pineridge Press, Swansea, U.K.

3. F. H. Harlow and A. A. Amsden, "A Numerical Fluid Dynamics Computational Method for All Flow Speeds," pp. 197-213 in Journal of Computational Physics, vol. 8, 1971.

4. L. D. Cloutman, C. W. Hirt, and N. C. Romero, SOLA-ICE: A Numerical Solution Algorithm for Transient Compressible Fluid Flows, Los Alamos National Laboratory, New Mexico, Report LA-6236, July 1976.

5. ASHRAE Handbook, 1977 Fundamentals Volume, American Society of Heating, Refrigerating and Air-Conditioning Engineers, Inc., New York, 1980.

6. W. H. McAdams, Heat Transmission, McGraw-Hill, New York, 1954.

7. Alan J. Chapman, Heat Transfer, MacMillan, New York, 1960.

APPENDIX

DESCRIPTION OF THE MODELS USED TO CALCULATE BOUNDARY TEMPERATURES AND HEAT TRANSFER FROM THE AMBIENT TO THE WALL CAVITY

For the analyses described in this report, it was convenient to divide the physical problem into two model problems, one for the heat transfer through solid boundaries and the other for the fluid flow within the wall cavity. After one fluids time step, the gas temperatures calculated in the fluids model provided boundary conditions for the heat transfer problem. Using those temperatures, a "steady-state" heat transfer solution was generated. Finally, the temperatures on the edges of the cavity were updated, providing boundary conditions for another time step in the fluids solution. In this appendix, the heat transfer model and the method used to couple the two analyses together are outlined.

The velocity boundary conditions for the fluid motion within the cavity (no slip and no flow at the surface) were applied as described in refs. 3,4. For the first case presented, in which the vertical cavity walls were maintained at different but constant temperatures, those temperatures were prescribed as boundary conditions on the energy equation.

To prescribe the wall temperatures in the more general non-isothermal case, the conduction problems within the solid building materials surrounding the cavity must be solved. The outer boundary condition for those conduction problems is convection across boundary layers to specified ambient temperatures. Because only steady-state results are of interest for the current problem, detailed calculation of the temperatures within the solid materials is not needed and, to minimize computing costs, should be avoided if possible.

To avoid calculation of detailed wall temperature distributions at each time step, the heat flow through the vertical walls was modeled as one-dimensional conduction. The thermal resistances of the material and the boundary layer next to the ambient temperature were used to calculate a lumped equivalent resistance for the composite. In this type of analysis one calculates temperatures at the "nodes" connecting the resistances. The network of thermal resistances and associated nodes is sketched in Fig. 9. By enforcing a heat balance on each node and equating the heat flux from the gas in the cavity with the heat flux through the composite wall, a linear relationship was developed between the gas temperature at the node nearest the edge of the cavity, the cavity edge temperature, and the specified ambient temperature. This expression was substituted for the boundary condition on the energy equation for the gas. Thus the local gas temperature was related directly to the local ambient temperature; and the detailed analysis of heat flow within the solids was bypassed, as desired. The essential one-dimensional assumption of this model is that conduction up and down the wall structures is negligible compared to conduction through the wall structures. Since the aspect ratio of the wall components is at least 96 to 1, this assumption seems justified.

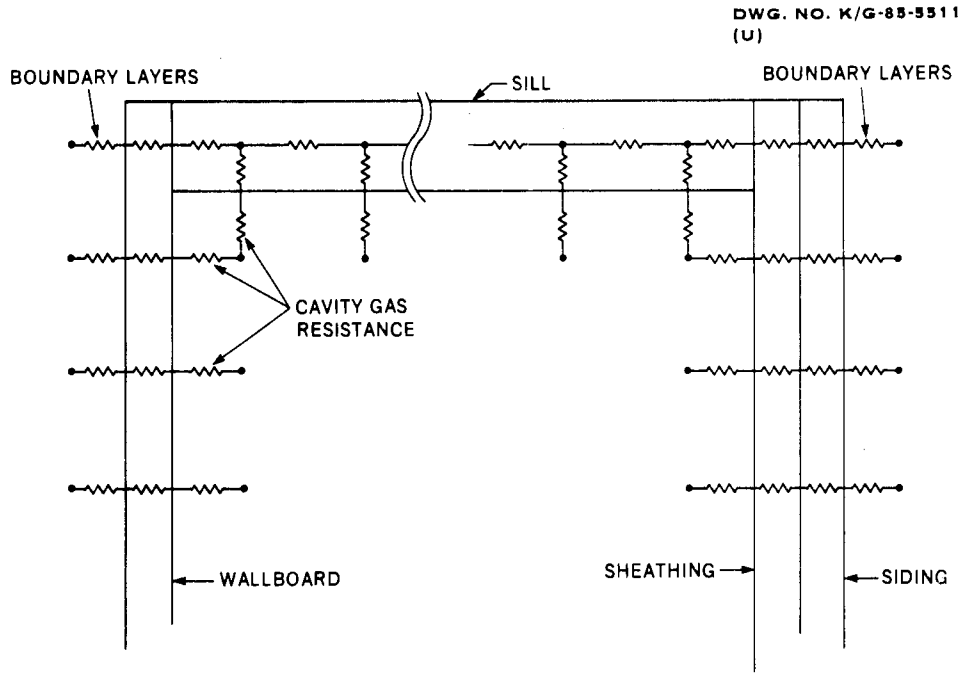

Fig. A.1. Schematic of thermal resistance network showing coupling from gas to cavity and ambient temperatures.

Heat flow in the sill plates at the top and bottom of the cavity can also be modeled using lumped parameter models, but the heat flow within the sills is two-dimensional. The sill and the conductance paths from the sill to the ambients were replaced with a network of equivalent thermal resistances. The network is sketched in Fig. A.1. By requiring that the heat flows into each node sum to zero, a system of linear equations was derived which relates the unknown sill nodal and edge temperatures to the ambient temperatures and the gas temperatures near the sill edges. An approximate linear relationship between each edge temperature and its nearest neighbor in the gas was generated by setting all other gas temperatures to their most recently calculated values. With this approximation, the gas temperature and edge temperature were coupled to the ambient temperatures in a linear fashion similar to that constructed for the vertical walls.

The lumped parameter models relating gas temperatures in the cavity directly to the specified ambient temperatures were substituted into the finite difference expressions for the conservation of energy in the computational cells next to the wall. Thus the fluid motion is controlled directly by the ambient conditions. Computationally, time saving implicit solution of the energy equation for the air in the cavity is justified since the driving boundary conditions can also be treated implicitly.

Radiant heat transfer between the walls and sills of the cavity was calculated using the Stefan-Boltzman equation and assuming that the surfaces were "gray bodies." The view factors were calculated using common methods of view factor algebra (ref. 7).

These equations describing the net thermal radiant transfer from the surface were linearized in the usual way, by factoring the fourth power of temperature terms into the product of linear and cubic parts. The resulting quasi-linear equations were combined with the conduction-convection models described in previous paragraphs, forming an energy balance about the surface node. These equations were used to couple the gas temperatures near the cavity walls to the ambient (driving) temperatures as described above.

Addition of radiant heat transfer to the system of quasi-linear equations couples the temperature of every surface node in the cavity to the temperature of every other. This system was uncoupled in the same way that the system of sill equations was uncoupled. Given the equation for any surface node, the temperatures at all of the gas nodes in the equation, except the nearest, were assigned the most recently calculated values. Since the coefficients in the "linear" equations were actually nonlinear functions of the surface temperatures, they were recalculated periodically. A gain in computational efficiency due to the quasi-linearization process resulted from careful scheduling of the linearization. Linearizing too often increased the computing cost and too seldom inhibited convergence of the computational process. The combination of periodic relinearization and approximate uncoupling of the linearized system of equations by lagging gas temperatures resulted in a cost effective, convergent solution technique for the heat transfer portion of the overall problem.

INTERNAL DISTRIBUTION

1. J. P. Belk
2. R. W. Browell
3. C. B. Bryan
4. D. W. Burton
5. R. S. Carlsmith
6-10. K. W. Childs
11. J. E. Christian
12. G. E. Courville
13. J. S. Crowell
14. R. C. DeLozier
15. J. B. Drake
16. R. G. Edwards
17. C. J. Emerson
18. W. Fulkerson
19. G. E. Giles
20. D. M. Hetrick
21. J. A. Hoffmeister
22. J. T. Holdeman
23. R. O. Johnson
24. W. S. Key
25. A. A. Khan
26-30. J. R. Kirkpatrick
31. W. F. Lawkins
32. D. W. Lee
33. G. H. Llewellyn
34. G. M. Ludtka
35. M. C. Matthews
36. B. E. McConnell
37. D. L. McElroy
38. P. W. McGrady
39. H. A. McLain
40. G. S. McNeilly
41. V. C. Mei
42. J. W. Michel
43. W. R. Mixon
44-48. J. E. Park
49. S. H. Park
50. M. R. Patterson
51. A. S. Quist
52. J. P. Sanders
53. M. Siman-Tov
54. A. Sozer
55. P. J. Steger
56. A. J. Szady
57. R. E. Textor
58. T. C. Tucker
59-63. J. N. Tunstall
64. R. C. Ward
65. T. D. Welch
66. G. E. Whitesides/R. P. Leinius/ Enrichment Technology Library
67. R. M. Widgeon
68. D. G. Wilson
69. Central Research Library (ORNL)
70. Document Reference Center (Y-12)
71. Enrichment Technology Library
72-73. Laboratory Records
74. Laboratory Records (RC)
75. ORNL Patent Office
76. Plant Records (RC)

EXTERNAL DISTRIBUTION

77. R. L. Alumbaugh, Naval Civil Engineering Laboratory, Port Hueneme, CA 93043
78. R. W. Anderson, 7090 Tecumesh Lane, Chanhassen, MN 55317
79. G. L. Askew, Tennessee Valley Authority, Chattanooga, TN 37402
80. C. D. Auburg, Department of Energy, Bonneville Power Admin., Portland, OR 97208
81. E. L. Bales, New Jersey Institute of Technology, Newark, NJ 07102
82. G. Barney, Portland Cement Association, Skokie, IL 60077

EXTERNAL DISTRIBUTION (continued)

83. J. R. Blasius, NO-TOX Products, Inc., Phoenix, AZ 85009
84. M. Bomberg, National Research Council of Canada, Ottawa, Canada
85. J. J. Boulin, Department of Energy, Washington, DC 20585
86. D. E. Brotherson, University of Illinois, Champaign, IL 61820
87. W. C. Brown, National Research Council of Canada, Ottawa, Canada
88. H. W. Busching, Clemson University, Clemson, SC 29631
89. R. Davis, 3073 Willoughby Road, Mason, MI 48854
90. A. O. Desjarlais, Dynatech Research and Development Company, Cambridge, MA 02139
91. R. S. Dougall, University of Pittsburgh, Pittsburgh, PA 15260
92. W. Gerken, Department of Energy, Washington, DC 20585
93. M. Gettings, Owens Corning Fiberglas, Granville, OH 43023
94. C. F. Gilbo, Journal of Thermal Insulation, Lancaster, PA 17602
95. L. R. Glicksman, Massachusetts Institute of Technology, Cambridge, MA 02139
96. W. P. Goss, University of Massachusetts, Amherst, MA 01003
97. E. I. Griggs, Tennessee Technological University, Cookeville, TN 38505
98. R. A. Grot, National Bureau of Standards, Gaithersburg, MD 20899
99. D. J. Harrje, Princeton University, Princeton, NJ 08540
100. M. Harton, Tennessee Valley Authority, Chattanooga, TN 37402
101. J. L. Heldenbrand, National Bureau of Standards, Gaithersburg, MD 20899
102. B. Howard, National Concrete Masonry Association, Herndon, VA 22070
103. C. W. Jennings, Tennessee Valley Authority, Chattanooga, TN 37402
104. J. Klems, Lawrence Berkeley Laboratory, Berkeley, CA 94720
105. F. Kubovich, Electra Manufacturing Corporation, Holland, OH 43528
106. R. A. Lacosse, National Roofing Contractors Association, Oak Park, IL 60631
107. M. D. Lyberg, Swedish Institute of Buildings, Box 785, Gavle, Sweden
108. P. C. Martin, Manville Service Corporation, Research and Development Center, Denver, CO 80217
109. D. McGuire, Regal Industries, Crothersville, IN 47229
110. K. Mentzer, Mineral Insulation Manufacturers Association, Summit, NJ 07901
111. G. Miller, Jim Walter Corporation, St. Petersburg, FL 33702
112. M. Millspaugh, Reflectixs, Inc., Markeville, IN 46056
113. M. Milne, University of California at Los Angeles, Los Angeles, CA 90024
114. M. P. Modera, Lawrence Berkeley Laboratory, Berkeley, CA 94720
115. P. G. Mulroney, VVKR, Inc., Alexandria, VA 22314
116. J. R. Mumaw, Owens Corning Fiberglas, Granville, OH 43023
117. R. E. Oliver, Department of Energy, Washington, DC 20585
118. L. Peterson, Thermoguard Insulation Co., Seattle, WA 98188
119. M. Reitz, New England Builder, Montpelier, VT 05602
120. J. Samos, NASA Langley Research Center, Hampton, VA 23665
121. S. Selkowitz, Lawrence Berkeley Laboratory, Berkeley, CA 94720
122. M. Sherman, Jim Walter Corporation, St. Petersburg, FL 33702
123. M. Sherman, Lawrence Berkeley Laboratory, Berkeley, CA 94720

EXTERNAL DISTRIBUTION (continued)

124. M. K. Snyder, Butler Manufacturing Company Research Center, Grandview, MO 64030
125. R. Sterling, University of Minnesota, Minneapolis, MN 55455
126. S. Tagore, Department of Energy, Washington, DC 20585
127. S. Taylor, Department of Energy, Washington, DC 20585
128. W. Tobiasson, United States Army CRREL, Hanover, NH 03755
129. T. W. Tong, Arizona State University, Tempe, AZ 85287
130. G. A. Tsongas, Portland State University, Portland, OR 97207
131. R. P. Tye, Dynatech Research and Development Company, Cambridge, MA 02139
132. J. R. Tyler, U. S. Fiber Corporation, Delphos, OH 45833
133. M. G. Van Geem, Portland Cement Association, Skokie, IL 60077
134. C. R. Vander Linden, Manville Service Corporation, Denver, CO 80217
135. J. R. Warner, American Consulting Engineering Counsel Research and Management Foundation, Washington, DC 20005
136. D. W. Yarbrough, Tennessee Technological University, Cookeville, TN 38505
137. R. Zarr, National Bureau of Standards, Gaithersburg, MD 20899
138. Office of Assistant Manager for Energy Research and Development, U. S. Department of Energy, Oak Ridge Operations, Oak Ridge, TN 37830
139-168. Office of Scientific and Technical Information, U. S. Department of Energy, P. O. Box 62, Oak Ridge, TN 37831